Forms of Hydraulic Fractures in Shallow Fine-Grained Formations

Lawrence C. Murdoch[1] and William W. Slack[2]

Abstract: Hydraulic fractures have been created in fine-grained formations at depths of 2–10 m to improve the performance of environmental remediation projects at dozens of locations and in a wide range of geologic conditions The effectiveness of a hydraulic fracture during remediation will depend primarily on its form; that is, its shape, thickness, orientation, length, width, and location with respect to the borehole The forms of many hydraulic fractures have been determined by mapping exposures in excavations and by compiling split-spoon sampling data These observations indicate that a typical hydraulic fracture at shallow depths is gently dipping, slightly elongate in plan, and slightly asymmetric with respect to the parent borehole Shallow hydraulic fractures lift the ground surface to produce gentle domes, and the pattern of uplift reflects the location and thickness of the fracture at depth The forms of hydraulic fractures created over a narrow range of depths at the same site are similar, but the forms can vary markedly between sites and at different depths at the same site This indicates that the forms of hydraulic fractures will be relatively consistent when they are created under similar conditions, but changes in geologic conditions can markedly affect fracture form.

DOI: 10.1061/(ASCE)1090-0241(2002)128:6(479)

CE Database keywords: Hydraulics; Fractures; Boreholes.

Introduction

Hydraulic fractures will be created in the vicinity of a borehole when fluid is injected at sufficient pressure This simple process can be either a blessing or a curse, depending on the application. Hydraulic fracturing has been used to improve the performance of oil and gas wells since the 1940s, and today it is a standard technique in the petroleum industry (Gidley et al. 1989). This application has been incredibly successful, increasing the extractable oil reserves of North America by 10^9 m^3 (Gidley et al. 1989) Other practioners are less enthusiastic about hydraulic fractures, however. Hydraulic fractures created during permeation or compaction grouting will affect the distribution of grout and can markedly reduce the ability of grout to seal or increase strength (Morgenstern and Vaughn 1963; Wong and Farmer 1973). Injection tests intended to determine the permeability of a formation are of limited value if hydraulic fractures are created near the well bore (Bjerrum et al. 1972).

Since the late 1980s (Murdoch 1988, 1989), hydraulic fractures have been created to augment a variety of procedures for remediating contaminated sites. Many of these sites are underlain by fine-grained formations where conventional methods of remediation are hampered by meager rates of fluid flow. Sand injected into hydraulic fractures in these materials will create lenses of high permeability material that can increase the specific capacities of wells by an order of magnitude or more (Murdoch et al. 1995) Recently, granules of reactive compound have been injected into hydraulic fractures to form in situ permeable barriers to contaminant migration (Murdoch 1995; Murdoch and Chen 1997; Murdoch 2000). When created normal to the direction of fluid flow, fractures filled with reactive material hold the potential for accelerating or augmenting the intrinsic remediation of fine-grained material. Other applications include filling hydraulic fractures with electrically conductive compounds, such as graphite, to enhance remediation by electrokinetics (Murdoch and Chen 1997; Chen and Murdoch 1999)

The effectiveness of a hydraulic fracture during remediation will depend primarily on its form; that is, its shape, thickness, orientation, length, width, and location with respect to the borehole. We have created hundreds of hydraulic fractures at shallow depths, and many of them have been explored to estimate their form in the subsurface. In several dozen cases the vicinity of the fracture was excavated to provide detailed cross sections (Murdoch 1995), whereas the exploration at other sites consisted of intersecting the fracture with a split-spoon or hand auger in several locations.

Details of the fracturing process and subsequent exploration efforts from 138 fractures at 13 sites were compiled in a database The database contains records describing fracture from with variables such as depth of initiation, dip, length of the major and minor axes, sand thickness, maximum uplift, and shape and volume of the displaced ground surface; as well as parameters of the fracturing operation, such as injected gel volume, bulk sand volume, slurry volume, maximum and minimum pressures, and whether the injected fluid reached the ground surface.

All hydraulic fractures that we created for environmental applications between 1989 and 1993 are included in this study. This provides a dataset of fracture characteristics resulting from similar procedures applied over relatively narrow ranges of depths,

[1]Assistant Professor, Dept. of Geological Sciences, Clemson Univ., Clemson, SC 29634 and President, FRx Inc., Cincinnati, OH. E-mail: lmurdoch@clemson.edu

[2]Vice President, FRx Inc., P.O. Box 498282, Cincinnati, OH 45249-8292. E-mail: bill@frx-inc.com

Note. Discussion open until November 1, 2002 Separate discussions must be submitted for individual papers. To extend the closing date by one month, a written request must be filed with the ASCE Managing Editor The manuscript for this paper was submitted for review and possible publication on September 6, 2000; approved on August 28, 2001. This paper is part of the ***Journal of Geotechnical and Geoenvironmental Engineering***, Vol. 128, No. 6, June 1, 2002 ©ASCE, ISSN 1090-0241/2002/6-479–487/$8.00+$.50 per page

and it includes test sites where most fractures were explored by either excavation or sampling.

Many other hydraulic fractures have been created since 1993, and the characteristics of most of them are well represented by the generalizations presented here. However, data describing the forms of hydraulic fractures created after 1993 are considerably sparser than the earlier data. Moreover, some applications since 1993 have involved creating hydraulic fractures over a wide range of depths at the same site, and this can cause marked changes in fracture form. In addition, methods for influencing the form of a hydraulic fracture were evaluated starting in 1994 (Murdoch et al. 1997). As a result, observations from after 1993 will be used to illustrate particular points, but we will rely on the earlier data for much of the evaluation.

The purpose of the following paper is to summarize the exploration data in order to characterize both the general features and essential details of hydraulic fractures created at shallow depths in fine-grained formations. Hydraulic fractures from one site were described in detail (Murdoch 1995), but a description of the general forms of shallow hydraulic fractures has never been published to our knowledge. The field observations will be presented at two levels of detail in the following paper. An idealized hydraulic fracture based on average values and typical responses from many field applications will be presented first. The idealized hydraulic fracture is a synthesis of many observations, and it is intended to form a conceptual model based on average values. This will be followed by descriptions of important features of hydraulic fractures based on observations from field sites where the features are particularly well exposed or documented. The latter section also contains summaries of statistics that highlight distributions of particular values. The information described here should provide practioners with guidelines about what to expect when creating hydraulic fractures at shallow depths, and it should provide modelers with an overview of features that could be predicted by theoretical analyses. The conceptual model described in the following pages is used as the basis for a mechanical analysis of shallow hydraulic fractures presented in a companion paper (Murdoch 2002).

Method of Hydraulic Fracturing

The process used to create hydraulic fractures described here begins by driving a casing to depth (Murdoch et al. 1995). Sediment at the bottom of the casing is exposed either by withdrawing a retractable point from within the casing or by driving an expendable point off the end of the casing. A water jet (18 L/min and 20 MPa) oriented normal to the axis of the casing is rotated to cut a disk-shaped cavity, or notch, in the exposed sediment. The water jet will create a notch 10–20 cm in radius in a few minutes in unlithified, fine-grained formations. Water is injected into the casing at a rate of 20–40 L/min, initiating a hydraulic fracture at the notch. A slurry of cross-linked guar gum gel and sand is injected into the fracture as it grows away from the borehole. An enzyme is added that reduces the apparent viscosity of the gel several hours after injection. The fracture closes when injection ceases and the gel flows into the soil mass, but the sand props the fracture walls open to provide a permanent layer of granular solids in the subsurface.

Monitoring the injection pressure and the displacement of the ground surface is a routine part of the fracturing procedure. The maximum injection pressure is typically one to a few hundred kPa at the onset of propagation, but the pressure decreased with time when most of the fractures described here where created. Ground displacements typically reach a maximum of 1 to 2 cm over the center of the fracture, and the displacement pattern resembles a gentle dome.

The fractures considered during this study were initiated at depths ranging from 1.4 to 12 m, and the average depth was 3 m. The average amount of sand injected into the fractures was 400 kg, although as much as 2,000 kg was injected into some fractures. The sand was injected at an average concentration of 1.2 kg sand/L gel, although concentrations ranged to as much as 1.8 kg/L. The volume ratio of sand in the slurry is the ratio (bulk volume of the packed sand)/(total volume of the slurry). The average volume ratio is 0.47 but it was as much 0.64 during this program.

Idealized Form

Shallow hydraulic fractures typically occur as one of two general forms depending on their average dip. One form is a steeply dipping fracture that has a greater vertical than lateral dimension. This type of fracture climbs rapidly and reaches the ground surface, or *vents*, in the vicinity of the borehole after a relatively small volume of liquid has been injected. Significant propagation ceases after venting has occurred. Thus it has been our experience that steeply dipping fractures in shallow sediments are of limited size and probably will result in limited improvement in the performance of vertical wells. As a result, little work has been done to characterize steeply dipping hydraulic fractures. Steeply dipping fractures were created at one site during the study period, but data from these fractures are not included here because exploration of their form was never conducted. Additional work is required to characterize the conditions that result in steeply dipping hydraulic fractures and the procedures for creating fractures under these conditions.

The other type of fracture form is gently dipping and it can grow to several meters or more in the horizontal dimension, which is large enough to improve the performance of shallow wells and therefore it is useful for environmental applications. Most of our investigation has focused on gently dipping fractures and they are the feature that will be described below.

An idealized model of a gently dipping hydraulic fracture has emerged from detailed mapping in excavations (Murdoch 1995) and interpretations from many other fractures explored in borings. The idealized hydraulic fracture created at shallow depths is slightly elongated in plan and dips back toward its parent borehole (Fig. 1). Most fractures develop a preferred direction of propagation and they extend furthest from the borehole in that direction. As a result, the center of the fracture in plan rarely coincides with the borehole. Instead, the center is displaced away from the borehole in the direction of preferred propagation (Fig. 1).

The database of fracture measurements provides typical values and ranges for the dimensions of shallow hydraulic fractures. The length of the major axis of the fracture, for example, is typically about three times greater than the depth of initiation, and the major axis of the fracture is 1.2 times greater than the minor axis (Fig. 2).

Important information about the dimensions of hydraulic fractures at depth comes from the pattern of displacement at the ground surface. Ground overlying the fracture is uplifted to create a gentle dome, and it appears that the displacement at the ground surface is similar to the aperture of a shallow fracture. The major

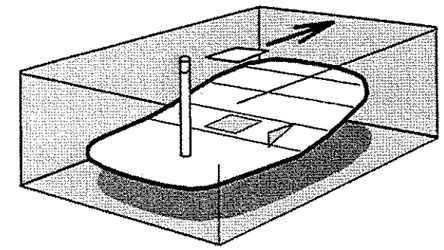

Fig. 1. Perspective of idealized gently dipping hydraulic fracture at shallow depth. Fracture dips toward parent borehole (triangle). Preferred direction of propagation (arrow) causes center of the fracture (square) to migrate away from the injection borehole.

axis of the dome ranges from 5 to more than 12 m, with an average of 8.5 m, and we infer that the underlying fractures were roughly these dimensions. The dome is typically slightly elongated with a mean aspect ratio of 6:5 (1.2:1). The borehole used to create the fracture and the point of maximum displacement (apex of the dome) rarely coincide with the center of the dome in plan. This eccentricity can be represented as the ratio (distance between the center of uplift and the borehole)/(major axis), *borehole eccentricity*, and the ratio (distance between the center of uplift and the point of maximum uplift)/(major axis), *displacement eccentricity*. Interestingly, the mean of both eccentricity values is 0.14. The borehole and the apex of the dome are typically on opposite sites of the center of uplift (Fig. 2).

The maximum uplift ranged from a few mm to more than 30 mm, with a mean of 18.8 mm. The fracture closes and the dome subsides after injection, but the injected sand prevents the fracture

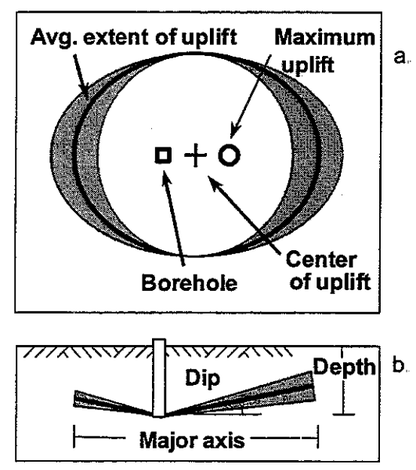

Fig. 2. Plan (a) and section (b) of a hydraulic fracture showing typical relative dimensions. Aspect ratio major:minor axis ranges from 1.0 to 1.4 (shaded) with a mean=1.2 (heavy black ellipse); major axis:depth mean=3.4; distance between borehole and center of uplift:major axis=0.14; distance between point of maximum uplift and center of uplift:major axis=0.14; fracture trace occurs within shaded triangular envelope with mean dip of 10°.

walls from closing completely. The amount of closure depends on the volume ratio of sand in the slurry, which is about 0.5 in most cases. As a result, the average thickness of sand in the fracture is about half of the maximum aperture when the fracture is inflated by pressurized slurry.

The idealized fracture has a preferred direction of propagation, and the line from the borehole through the point of maximum uplift indicates that direction. With prolonged injection, the fracture will reach the ground surface along that line. The preferred direction of propagation is commonly related to distribution of vertical load at the ground surface, with the fractures propagating toward regions of diminished vertical load. Beneath sloping ground, therefore, it is possible to anticipate the preferred direction: it is typically downslope. Beneath level ground we have used vehicles to artificially load the ground surface and influence the propagation direction away from the vehicles (Murdoch 1995).

In cross section, some fractures were nearly flat-lying in the vicinity of the borehole and they curved gradually upward to form a basin-like form, whereas in other cases the fractures appear to maintain a roughly uniform dip from the borehole to their termination (Murdoch 1995). Fracture traces commonly appear to be step-like, changing dip over several dm when mapped in detail on the wall of a trench (Murdoch 1995). As a result, we are unable to present a curve that characterizes the range of details of fracture traces in cross section. Instead, we use an envelope [shaded triangle in Fig. 2(b)] that spans a range of dips with the understanding that the fracture trace occurs somewhere within that envelope.

We compared the dips of fractures and found that the average values ranged from 5° to 25° at different sites. At each particular site, however, the dips were more consistent, with the 95% confidence interval of dips approximately 5°. Moreover, the dips at some sites were statistically different from dips at other sites, so that dip angle appears to depend on site conditions. The heavy line in Fig. 2 dips 10°, which is approximately the average dip of fractures created during this study. The triangular envelope in Fig. 2(b) bisects an angle of 10°, which is twice the 95% confidence interval of dips at individual sites.

Important Characteristics

Essential characteristics of fracture form were identified by reviewing data from field observations. In addition to mean values of characteristics cited above, the data also provide insights into the range of observed forms and other characteristics that were used to infer the idealized forms in Figs. 1 and 2. The following section contains a review of the observed dips of hydraulic fractures, as well as the depth of initiation and the distribution of displacement along the major axis of the fracture. Observations of the transient changes in fracture aperture and displacement of the ground surface are presented, followed by a detailed description of the patterns of net displacement over hydraulic fractures.

Dip

True and apparent dip (or inclination) of 90 hydraulic fractures are known from excavation studies and from locations where fractures were intersected in samples obtained by boring at 10 sites. In most cases, the fracture surface dips toward the borehole, so the apparent dip is similar to the true dip averaged between the borehole and the sampling point. Where fractures were sampled at several locations along a radial line, the apparent dip provided by each sample was averaged to estimate the dip along that line.

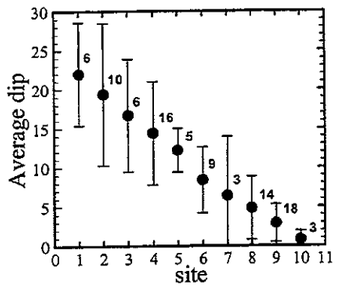

Fig. 3. Dips of hydraulic fractures at ten sites underlain by silty clay. Error bars are 95% confidence intervals and the number of fractures measured at each site are shown next to the data points. All but two of the sites are underlain by silty clay glacial drift; No. 4 is underlain by a vertisol, and No. 10 is underlain by interbedded clay, silt, and fine-grained sand of fluvial origin. Site No. 2 is within 100 m in plan and is 10 m stratigraphically below site No. 9.

In general, the mean dips of fractures at any particular site range from 0.8 to 22°, and 95% confidence intervals range from 3.0 to 8.2° (Fig. 3). The mean confidence interval is 4.4 ± 1.08°.

The mean dips of fractures were compared using the Student-Neuman-Keuls test with 95% confidence (Glantz 1992). This analysis shows that the dips of fractures at sites where the mean dip was gentle are statistically different from dips at sites where fractures dip relatively steeply. Moreover, fracture dips at the intermediate sites are statistically different from both the shallow and steep end members.

This result is intuitively appealing based on Fig. 3, and it indicates that the dip of a hydraulic fracture depends on site conditions. At a particular site where the geology is uniform laterally, however, the dips are fractures that are relatively uniform, within roughly 5° of the mean dip for that site.

Depth

Hydraulic fractures were created from depths as shallow as 1 m to as deep as 12 m during this program. Most theoretical analyses of shallow hydraulic fractures regard interaction with the ground surface as a fundamental process affecting growth, with the ratio of fracture length to depth being a basic measure of the interaction (Pollard and Holzhausen 1979). The ratio of the major axis to the depth for 99 fractures created during this program ranges from 1.5 to greater than 5.5, with an average of 3.4 and a median of 3.2. That ratio is 3.0 or more for 79% of the fractures (Fig. 4). This ratio may partly reflect the volume of fluid injected into each fracture, and different ratios may result when different volumes are injected.

Distribution of Sand and Uplift along Major Axis

The distribution of sand is a critical factor when fractures are used to improve remediation. Deformation of the ground surface is related to the location and aperture of a hydraulic fracture at depth (Davis 1983; Holzhauzen et al. 1985), which in turn should be related to the distribution of sand within a fracture. The details of those relations were investigated by comparing uplift to fracture aperture at the point of injection, and by comparing uplift to the distribution of sand in a fracture.

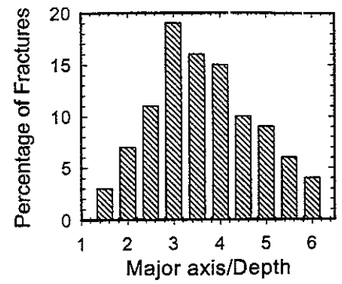

Fig. 4. Distribution of ratio between major axis and depth of initiation of hydraulic fractures

The thickness of sand was measured at 15-cm intervals along 19 fractures revealed in the walls of trenches, and net uplift was measured along the lines of the trenches when the fractures were created at the ELDA landfill in Cincinnati, Ohio. The data show that the thickest point of the fracture is typically near the midpoint between the fracture ends. However, all the fractures grew to greater lengths in one direction compared to other directions from the borehole. For example, in Fig. 5, sand filling the fracture extends 5 m in one direction but only 3 m in the opposite direction. As a result, the point of injection was skewed toward one end of the fracture and the thickest part of the fracture never coincided with the point of injection.

A wide range of variability in sand thickness characterized all of the fractures (Fig. 5). For example, the thickness of sand in the fractures commonly ranged from 50% more to 50% less than the thickness indicated by a regression line. This variability in thickness occurred as the fracture pinches and swells over distances of a few dm to a few cm along the fracture trace.

A regression line through the sand-thickness data mimics the pattern of uplift, although the sand thickness is typically about half the uplift value (Fig. 5). The volume ratio of sand in the slurry injected into this fracture was 0.5. It appears that the ratio between the uplift and average sand thickness is similar to the volume ratio of sand in the slurry, although there is significant variability in the sand thickness. This is significant because it suggests that the average thickness of sand in shallow, flat-lying fractures can be roughly estimated as the product of the uplift and the volume ratio of sand in the slurry.

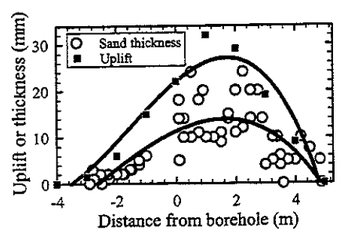

Fig. 5. Thickness of sand along two sides of trench cutting the major axis of a fracture and the net uplift immediately after injection as a function of distance from the borehole. Volume ratio of sand in the injected slurry was 0.5. Heavy lines are third-order regression polynomials.

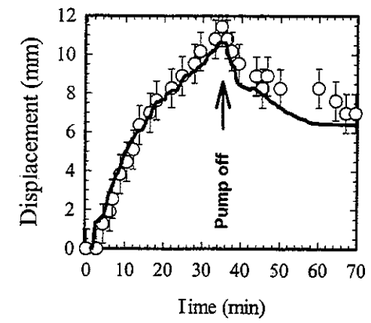

Fig. 6. Uplift (symbols) of the ground surface measured with telescope and fracture aperture (line) measured with borehole extensiometer

Hydraulic fractures at the ELDA Landfill where created on a topographic bench and the preferred direction of propagation was toward the cut edge of the bench. Pollard and Muller (1976) show that the shape of a sheet intrusion will resemble a tear drop, which is similar to Fig. 5, in the presence of a regional gradient in confining stress. We expect that the vertical gradient imposed by the bench influenced the forms of the hydraulic fractures at the EDLA site, much like a regional gradient affects the forms of sheet intrusions. Interestingly, the actual thickness of sheet intrusions varies locally from the tear drop form (Pollard and Muller 1976; Figs. 2 and 3), much like the thickness of the hydraulic fracture varies in Fig. 5.

Fracture Aperture and Uplift at Borehole

Fracture aperture was measured as a function of time using a borehole extensiometer, which consists of a fine wire that was anchored to the lower wall of a fracture and extended upward through a cased bore to the ground surface. The wire passed through a pressure-tight seal at the top of the casing and was fixed to a displacement transducer. As the fracture opened, the wire was pulled into the casing by an amount equal to the aperture of the fracture. A graduated scale was fixed to the casing at the ground surface and the uplift was determined as the difference between repeat measurements made with a leveling telescope.

The results show that both fracture aperture and uplift increase with time during injection, and the rate of increase of both diminishes with time (Fig. 6). After pumping, both aperture and uplift decrease to approximately 0.5–0.7 of the maximum value. Not only do aperture and uplift show the same behavior, they show essentially the same values during both opening and closing of the fracture. It appears that measurements of uplift at the point of injection will serve as reasonable estimates of fracture aperture beneath that point, at least for a shallow fracture within a few m depth. In contrast, uplift can be smaller in magnitude and greater in extent than the aperture of a flat-lying fracture that is relatively deep (Pollard and Holzhauzen 1979).

Those comparisons, combined with the observations described above, have led to the following conclusions:

- The aperture of a flat-lying, shallow hydraulic fracture is roughly equal to the uplift overlying the fracture at the time injection is terminated;
- The average thickness of sand in the fracture is equal to the aperture times a correction factor, which is related to the fraction of sand in the injected slurry;

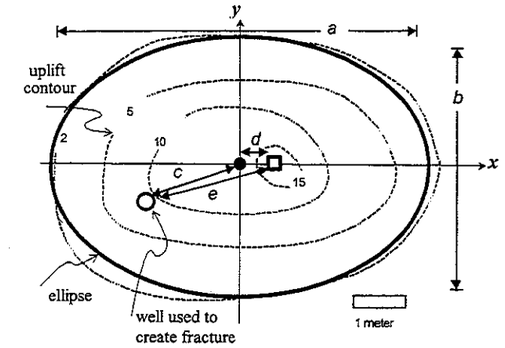

Fig. 7. Stylized uplift contours (dashed lines) in mm with ellipse used to characterize the pattern (thick line). Bar scale is roughly 1 m. *a*: major axis of ellipse; *b*: minor axis of ellipse; *c*: distance from the center of the ellipse to the well used to create fracture (open circle); *d*: distance from the center to the point of maximum uplift; and *e*: distance from the well to the point of maximum uplift.

- The correction factor is equal to the volume ratio of sand in the slurry where the uplift is greater than 2 to 3 mm. This assumes that negligible liquid has leaked out of the fracture during injection and that the fracture is inflated by the injected volume of slurry at the time fracturing stops. The liquid phase of the slurry flows out of the fracture and the overburden subsides until it is supported by the injected sand;
- Sand appears to be absent from the leading edges of hydraulic fractures, so the correction factor is zero where the uplift is less than 2 to 3 mm. This may be because the leading edge of the fracture is too narrow to accept coarse sand grains (1 mm diameter);
- The thickness of sand is highly variable (±50%) so that large differences between the thickness observed in point samples, from a split-spoon sample, for example, and that estimated using uplift should be expected. Likewise, samples obtained within a few dm may yield marked differences in thickness of sand; and
- The simplified relationships between uplift and sand thickness cited above are limited to fractures that dip less than approximately 35°, and where the maximum length of the fracture is greater than the depth.

Pattern of Uplift

The pattern of uplift appears to be the best estimate of the distribution of sand in a shallow hydraulic fracture that is readily available. This pattern can be quickly measured in the field using simple leveling equipment, and such measurements are available for most fractures created during this study. We have quantified the general pattern of uplift for all the fractures where we have data in order to evaluate common characteristics. This was done by assuming that the uplift pattern resembles an elliptical dome, which is a reasonable assumption for the majority of the fractures. The boundaries of an ellipse were manually fit to the 2 mm contour of uplift (Fig. 7) to mark the area inferred to contain sand. In most cases the ellipse fit the uplift pattern well within the error associated with interpolation of the uplift field. The axes of the ellipse were used to define a coordinate system, with the major

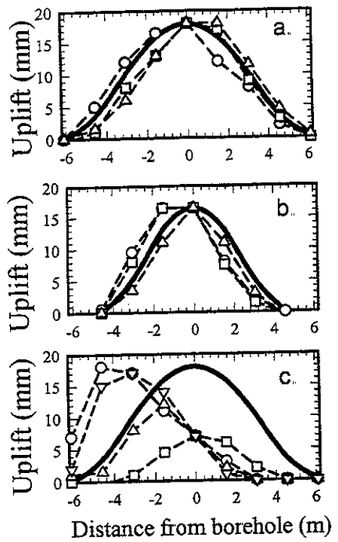

Fig. 8. Uplift as a function of distance from the borehole for three fractures created at shallow depths in silty clay. Uplift was measured at stations (points) along three (a and b) or four (c) lines in the field. The heavy line is a fourth-order polynomial used in a theoretical analysis presented by Murdoch (2002).

axis along the x axis. The locations of the point of maximum uplift and the point of injection were located using that coordinate system (Fig. 6).

Several common methods of interpolation were evaluated by comparing the estimated and exact volumes beneath an idealized dome that resembles the uplift pattern over a hydraulic fracture. Kriging with a linear variogram produced the least error and it was used to interpolate all the uplift fields prepared for this work.

Shape of Surface

The uplifted surface forms a dome that ranges from nearly symmetric to highly asymmetric with respect to the point of injection. The uplift pattern is nearly identical along the six radial lines of observation points overlying a nearly symmetric fracture [Fig. 8(a)], whereas they differ markedly as the degree of asymmetry increases [Figs. 8(b and c)]. The uplift along the major axis of an asymmetric fracture is tear-drop shaped, with a gradual taper from the point of maximum thickness to the borehole and a sharp taper in the opposite direction. In contrast, the uplift along the minor axis [square symbols in Fig. 8(c)] is nearly symmetric.

Asymmetric uplift occurs over a fracture that is dipping, with the strike of the fracture plane along the minor plan axis and the dip direction along the line from the point of maximum uplift to the borehole. The dip direction of fractures shown in Figs. 8(b and c) lies along the lines indicated by circles, and the fractures are shallowest on the left side of the diagram and deepest on the right side.

A total of 74 fractures were used to characterize ground surface displacements, and the results are summarized in Table 1. Data from steeply dipping fractures were omitted because the displacements were difficult to characterize using available methods. In general, all the data are skewed to the right (Table 1). The degree of skewedness is minor, however, so the arithmetic mean will be used to characterize typical values.

The displacement of the ground overlying hydraulic fractures created during this study formed a slightly elongated dome with circularity that is typically 1.2 [Fig. 9(a)] and never more than 1.73.

The borehole and the point of maximum uplift are generally within about 15%, and never more than 35% of the major axis from the center of the dome, as indicated by values of borehole and displacement eccentricities [Figs. 9(b and c)]. The distances between the borehole and the point of maximum uplift [borehole offset, Fig. 9(d)] is greater than either of the eccentricity values, with an average of 20% and a maximum of 60% of the major axis. It follows that, in general, the borehole is on one side and the maximum uplift is on the other side of the center of uplift.

The borehole eccentricity is related to the chance that the fracture will reach the ground surface (vent). The percentage of fractures that vent increases from between 5 and 10% to between 25 and 30% as eccentricity increases to 0.3, and all the fractures with borehole eccentricity greater than 0.3 vented to the ground surface [Fig. 9(e)].

Asymmetry of the fracture surface is an important indicator of the fracture at depth. Gently dipping hydraulic fractures commonly develop a preferred direction of propagation that is coincident with the direction of asymmetry in the uplift surface. The fractures climb in the direction of propagation and the degree of asymmetry will increase as a fracture approaches the ground surface.

Volumes of Displacement

The ground overlying a hydraulic fracture displaces upward as fluid is injected during fracturing, and the volume represented by the displacement is expected to be related to the volume of injected slurry (liquid+solid volume). Volumes of displacement were determined by interpolating between the points of measured uplift to estimate a continuous surface describing the displacement, and then integrating the volume under that surface. The interpolation and integration were done using *SURFER*, a commercially available software package.

The displaced volumes are either approximately equal to or slightly less than the actual volumes of injected slurry. A first order regression of the displaced and actual volumes yields a line with a slope of 0.98 and a correlation coefficient of 0.79. The residual between the estimated uplift volume and the volume predicted by the linear fit is within the field measurement error (0.07 m^3) for 50% of the data. It appears that the volume displaced by the ground surface is roughly equal to the volume injected for about half the hydraulic fractures and it is less than the injected volume for the other half. The volume of the uplifted surface can be considerably less than the injected volume when hydraulic fractures vent to the surface, or when they are relatively steep but remain confined within the subsurface. A ratio of volume uplift:injected volume that is considerably less than 1.0 can be used as an indicator of problems, either related to venting or to the creation of steeply dipping fractures.

Table 1. Statistical Parameters Describing Surface Deformation

	Mean $\bar{x}$	Median M_e	Mode M_0	Maximum	Minimum	Standard deviation σ	Skewness[a]
Circularity	1.21	1.18	1.2	1.73	1.0	0.16	0.59
Borehole eccentricity	0.14	0.14	0.1	0.32	0	0.08	0.12
Displacement eccentricity	0.14	0.12	0.1	0.34	0	0.09	0.67
Borehole offset	0.22	0.20	0.2	0.61	0	0.15	0.38

[a]Pearsons coefficient of skewness: $3(\bar{x}-M_e)/\sigma$.

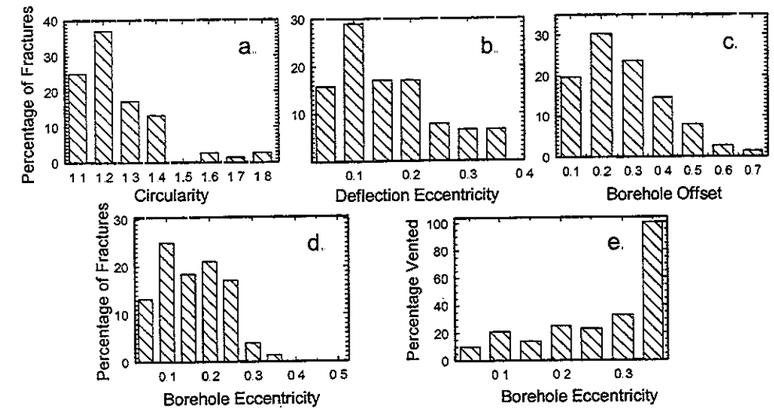

Fig. 9. Observed characteristics of uplift pattern over hydraulic fractures based on definitions in Fig. 7

Surface Cracking

Dilational cracks may form at the ground surface in areas overlying shallow hydraulic fractures. The extent and pattern of cracking is highly dependent on the type of material at the ground surface; surface cracks are best developed beneath dry bare soil, but they may be difficult to detect beneath grass. Existing cracks in concrete slabs or pavement can be dilated by an underlying hydraulic fracture.

Surface cracking is characterized by one to several fractures that are nearly vertical with roughly radial orientations and are accompanied by many smaller cracks forming polygonal patterns. Surface cracks typically have apertures of a few mm, but some may gap open by more than one cm. The numbers and apertures of surface cracks are always greatest beneath the point of maximum uplift, and they increase with the magnitude of uplift. Indeed, inspection of the surface cracks during injection can often be used to forecast the location of the point of maximum uplift (Fig. 7) and the preferred propagation direction.

The number and spacing of surface cracks is greatest at the apex of the uplifted dome, and the area containing surface cracks is roughly defined by an uplift contour that is approximately 0.5 of the uplift at the apex. Cracks never occur near the margins of the uplifted area, and the occurrence of surface cracks appears to be unrelated to venting of injected fluid to the ground surface.

The aperture of surface cracks is greatest immediately after all fluid has been injected, and it decreases with time as the ground surface subsides after injection. We have pushed thin rods into the cracks to estimate their depth, and all of them appear to have negligible aperture below about 0.5 m. Injected slurry rarely flows out of the surface cracks, so it appears that the surface cracks terminate above the pressurized hydraulic fracture.

Discussion

Hydraulic fractures can be created in all the materials that we have tested. This includes glacial drift throughout the Midwest and New England; swelling clays near Beaumont and Dallas, Tex.; residuum on limestone; saprolite in South Carolina and Pennsylvania; interbedded fine to medium-grained alluvium in Nebraska, Texas, South Carolina, and New Mexico; and lithified sedimentary rock in the vicinity of Denver. Based on those results, it is expected that hydraulic fractures can be *created* in any fine-grained earthen material. Laboratory results show that hydraulic fractures can even be created in clay-rich slurry.

Even though hydraulic fractures can be created in many formations, whether they are *useful* is another issue. Nearly all of the hydraulic fractures created during this program have been intended to improve the effectiveness of environmental remediation. The permeability of the formations mentioned above is low, so sand was injected into many of the hydraulic fractures to create permeable layers intended to increase the performance of wells. The geometry of a hydraulic fracture is an important aspect of how it affects well performance. Fractures that are gently dipping are the most useful because at shallow depths they can be larger than fractures that are steeply dipping. This is simply because steeply dipping hydraulic fractures may reach the ground surface while they are still quite small. Some applications, such as vapor extraction that draws air downward from the ground surface, will benefit from the flow paths induced by gently dipping hydraulic fractures and may be adversely affected by steeply dipping fractures.

The state of stress and the degree of layering in subsurface material appear to be the most important factors affecting the orientation of hydraulic fractures at shallow depths. A relatively high horizontal compressive stress certainly favors the creation of hydraulic fractures that are gently dipping (Murdoch 1995). However, nearly flat-lying hydraulic fractures have been created at several sites underlain by interbedded sediments that were soft and assumed to be normally consolidated. We expected that the

direction of maximum compression was vertical at these sites and it appears that the orientation of hydraulic fractures was influenced more by the material layering than the state of stress. At sites where we have observed hydraulic fractures to be steeply dipping, the subsurface consists of massive, or unstructured materials where the vertical compressive stress is probably greater than the horizontal stress.

The effects of state of stress and material layering are difficult to quantify at this time because field data measuring these properties are sparse from sites where hydraulic fracturing tests have been conducted (Murdoch 1995). One reason for this is that nearly all of the hydraulic fractures have been created at environmental sites, and the lateral earth pressure is rarely measured during characterization of these sites. Moreover, the costs of conducting tests to measure in situ stress are difficult to support because their importance to remediation has been difficult to justify for applications other than hydraulic fracturing. The other reason is that a method for measuring the horizontal and vertical fracture toughness in sediment, which would be required to characterize the effect of layering on fracture orientation, is currently unavailable.

It is possible to use published information to anticipate the occurrence of overconsolidated sediments. For example, Mahar and O'Neill (1983) show that K_0 (ratio of lateral to vertical stress) in Beaumont soils, a montmorillonite-rich vertisol that occurs in the vicinity of Houston, are greater than 1.0 at depths less than 10 m. Hydraulic fractures created in similar materials near Beaumont, Tex. had an average dip of approximately 14° (location 4 in Fig. 3), and we expect that this gentle dip was controlled by the stress in the soil. Maps of soil type [e.g., USGS Sheet 86 (1967) or local soil surveys] can be used to anticipate the occurrence of some shallow, overconsolidated materials.

Forms of hydraulic fractures created at similar depths at a particular site are generally similar, but forms of fractures created at different depths may be quite different. For example, hydraulic fractures were created at depths ranging from 2 to more than 10 m at two sites underlain by silty clay till. Fractures created between 2 and 4 m depth resembled Fig. 1 with dips of roughly 15°. The dips of the hydraulic fractures increased with depth, however, and most of the deepest ones dipped steeply (more than 70°), according to the results of sampling efforts after the fractures were created. Curiously, two deep fractures were discovered that were gently dipping, even though most of them dipped steeply.

The state of stress at those two sites is unknown, however, many fine-grained deposits are overconsolidated (with a relatively large horizontal compression implied) at depths less than 3 or 5 m and are normally consolidated (with a large vertical compression implied) at greater depths (Soderman and Kim 1970; Mahar and O'Neill 1983). This type of change in state of stress would explain the change in fracture orientation with depth that was observed at the two sites underlain by till.

Stratigraphic layering will also affect how fracture form may change with depth. For example, hydraulic fractures were created at two sites underlain by interbedded fine-grained sand, silt, and clay in the flood plains of major rivers. The sediment was saturated and quite soft at both sites and we assume that it was normally consolidated although geotechnical data are unavailable. The state of stress implied by the assumed consolidation led us to expect that hydraulic fractures would dip steeply at both sites; however, this was not the case. Hydraulic fractures at one site were flat-lying, essentially parallel to bedding, from 2 to 12 m depth. At the other site, the dips of fractures varied markedly with depth; they dipped steeply at shallow depths, but were flat-lying at depths between 5 and 8 m. A bed of finely laminated silty clay occurred from 5 to 8 m, and the hydraulic fractures were parallel to the laminations. Vertical fractures were created in the overlying sediments, which were relatively massive.

Hydraulic fractures created by other investigators appear to be consistent with the characteristics presented here, even though some of the geologic settings differ from the ones described here. For example, hydraulic fractures created in saprolite derived from granitic gneiss in Georgia are gently dipping and slightly elongate, generally resembling Fig. 1, according to Frere and Baker (1995). Grout injected to reinforce a slope underlain by silty clay apparently resulted in roughly flat-lying hydraulic fractures (Chandler 1997).

Conclusion

Several hundred hydraulic fractures have been created by injecting slurry at shallow depths (less than 10 m) in fine-grained formations from a wide range of geologic settings. A gently dipping form that is slightly elongate and asymmetric with respect to the injection boring (Fig. 1) characterizes many of these fractures. Hydraulic fractures dip toward their parent borehole, and the mean value of the dip is about 10°. The dip, or inclination of the fractures, ranges from roughly 0° to more than 20°. Steeply dipping fractures were created in a few cases, but they are uncommon. The aspect ratio of fractures in plan view has a mean of 6:5, but it can be nearly unity and it is rarely more than 7:5. The long axis of the fracture is roughly parallel to the dip direction.

The major axis of most fractures is typically three times greater than the depth of initiation, and this ratio ranges from greater than 2 to less than 6. This ratio is significant because it determines the extent to which a fracture can lift its overburden; the overburden can be lifted when the ratio is greater than 2 to 3, whereas the fracture opens by compressing the overburden when the ratio is less than 1.0 (Pollard and Holzhausen 1979; Murdoch 1995). Accordingly, most fractures created during this program probably opened by lifting their overburden.

The effect of lifting the overburden is manifested in other ways, such as the relationship between uplift, aperture, and sand thickness. Field measurements suggest that the inflated aperture of a shallow hydraulic fracture is similar to the uplift. The average thickness of sand carried into the fracture appears to be a fraction of the inflated aperture, and that fraction is roughly equal to the volume ratio of sand in the injected slurry. These findings probably will differ for fractures that are relatively deep (the ratio of major axis to depth is less than 1) or that dip significantly (greater than 35°). In those cases, the pattern of displacement at the ground surface can be significantly different than the fracture aperture (Pollard and Holzhausen 1979), and more more sophisticated analyses are required to predict the distribution of sand filling a hydraulic fracture (Davis 1983; Holzhausen et al. 1985; Du et al. 1993).

The general form of fractures created over a depth range of a few m at the same site is similar, however, there can be a significant range in forms among fractures created at different sites and at different depths within the same site. Stratigraphic layering, along with the state of stress and the anisotropy in fracture toughness appear to be important controls of fracture form based on mechanical arguments (Murdoch 1993a,b,c; Harison et al. 1994; Murdoch 1995). Field data documenting the state of stress and fracture toughness are unavailable for most of the sites where we created hydraulic fractures, so additional work is required before the form of a hydraulic fracture can be predicted based on site conditions alone.

The results of this study indicate that the forms of hydraulic fractures will be relatively consistent when they are created under similar conditions. This finding is important to the useful application of hydraulic fractures because it indicates that the form of a fracture can be anticipated based on results from similar conditions; that is, the fractures created at one location will be similar to those created at nearby locations where the geologic conditions are similar.

The general characteristics identified in the previous pages should be a target for efforts that attempt to predict how hydraulic fractures behave at shallow depths. Some of those characteristics can be explained in a theoretical model that will be described in a companion paper (Murdoch 2002).

Acknowledgments

The writers appreciate the support of the National Science Foundation (EAR9876124) and the U.S. Environmental Protection Agency (68-03-3379-08; CR-822677).

References

Bjerrum, L., Nash, J. K. L., Kennard, R. M., and Gibson, R. E. (1972). "Hydraulic fracturing in field permeability testing." *Geotechnique*, 22, 319–332.

Chandler, S. C. (1997). "Lense grouting with fiber admixture to reinforce soil." *Grouting: Compaction, remediation and testing*, ASCE, New York, 147–157.

Chen, J-L., and Murdoch, L. C. (1999). "Effects of electroosmosis on natural soil: Field test." *J. Geotech. Geoenviron. Eng.*, 125(12), 1090–1098.

Davis, P. M. (1983). "Surface deformation associated with a dipping hydrofracture." *J. Geophys. Res., [Space Phys.]*, 88, 5826–5834.

Du, Y., Aydin, A., and Murdoch, L. C. (1993). "Incremental growth of a shallow hydraulic fracture at a waste remediation site, Oakbrook, Illinois from inversion of elevation changes." *Int. J. Rock Mech. Min. Sci. Geomech. Abstr.*, 30(7), 1273–1279.

Frere, J. M., and Baker, J. E. (1995). "Use of soil fracturing to enhance soil vapor extraction, a case study." *Emerging technologies in hazardous waste management VII*, American Chemical Society, Atlanta, GA.

Gidley, J. L., Holditch, S. A., Nierode, D. E., and Veatch, R. W. (1989). *Recent advances in hydraulic fracturing*. Society Petroleum Engineers Monograph. 452.

Glantz, S. A. (1992). *Primer of biostatistics*, 3rd Ed., McGraw-Hill, New York, 440.

Harison, J. A., Hardin, B. O., and Mahboub, K. (1994). "Fracture toughness of compacted cohesive soils using a ring test." *J. Geotech. Eng.*, 120(5), 872–891.

Holzhausen, G. R., Haase, C. S., Stow, S. H., and Gazonas, G. (1985). "Hydraulic-fracture growth in dipping anisotropic strata as viewed through the surface deformation field." *Proc., 26th U.S. Symposium on Rock Mechanics*, Rapid City, SD.

Mahar, L. J., and O'Neill, M. W. (1983). "Geotechnical characterization of dessicated clay." *J. Geotech. Eng.* 109(1), 56–71.

Morgenstern, N. R., and Vaughan, P. R. (1963). "Some observations on allowable grouting pressures." *Proc., Conf. Grouts and Drill Muds*, Institute of Civil Engineering, London, 36–42.

Murdoch, L. C. (1988). "Innovative delivery and recovery using hydraulic fracturing." *Proc., 14th Annual USEPA Research Symposium*, 613.

Murdoch, L. C. (1989). "A field test of hydraulically fracturing glacial till." *Proc., 15th Annual USEPA Research Symposium*, Cincinnati.

Murdoch, L. C. (1993a). "Hydraulic fracturing of soil during laboratory experiments: methods and observations." *Geotechnique*, 43(2), 255–265.

Murdoch, L. C. (1993b). "Hydraulic fracturing of soil during laboratory experiments: propagation." *Geotechnique*, 43(2), 266–276.

Murdoch, L. C. (1993c). "Hydraulic fracturing of soil during laboratory experiments: theoretical analysis." *Geotechnique*, 43(2), 277–287.

Murdoch, L. C. (1995). "Forms of hydraulic fractures created during a field test in fine-grained glacial drift." *Q. J. Eng. Geol.*, 28, 23–35.

Murdoch, L. C. (2000). "Remediation of organic chemicals in the vadose zone." *Vadose Zone, Science and Technology Solutions*, B. B. Looney and R. W. Falta, eds., Battelle, 1540.

Murdoch, L. C. (2002). "Mechanical analysis of idealized shallow hydraulic fracture." *J. Geotech. Geoenviron. Eng.*, 128(6), 488–495.

Murdoch, L. C., and Chen, J-L. (1997). "Effects of conductive fractures during in situ electroosmosis." *J. Hazardous Mater.*, 55, 239–262.

Murdoch, L. C., Slack, W., Siegrist, R., Vesper, S., and Meiggs, T. (1997). "Advanced hydraulic fracturing methods to create in situ reactive barriers." *Proc., Int. Containment Technology Conf. and Exhibition*, St. Petersburg, Fla.

Murdoch, L. C., Wilson, D., Savage, K., Slack, W., and Uber, J. (1995). *Alternative methods for fluid delivery and recovery*. USEPA/625/R-94/003.

Pollard, D. D., and Holzhausen, G. (1979). "On the mechanical interaction between a fluid-filled fracture and the earth's surface." *Tectonophysics*, 53, 27–57.

Pollard, D. D., and Muller, O. H. (1976). "The effect of gradients in regional stress and magma pressure on the form of sheet intrusions in cross section." *J. Geophys. Res.*, 81(5), 975–983.

Soderman, L. G., and Kim, Y. D. (1970). "Effect of groundwater levels on stress history of the St. Clair clay till deposit." *Can. Geotech. J.*, 7, 173–187.

USGS Sheet 86. (1967). *Distribution of principal kinds of soils: orders, suborders, and great groups*.

Wong, H. Y., and Farmer, I. W. (1973). "Hydrofracture mechanisms in rock during pressure grouting." *Rock Mech.* 5, 21–41.